Journal of Inorganic Biochemistry 195 (2019) 20–30

Contents lists available at ScienceDirect

Journal of Inorganic Biochemistry

journal homepage: www.elsevier.com/locate/jinorgbio

Stability constant determination of sulfur and selenium amino acids with Cu(II) and Fe(II)

Jaime M. Murphy[a], Andrea A.E. Gaertner[a], Tyler Williams[a], Colin D. McMillen[a], Brian A. Powell[a,b], Julia L. Brumaghim[a,*]

[a] Department of Chemistry, Clemson University, Clemson, SC 29634-0973, USA
[b] Department of Environmental Engineering and Earth Sciences, Clemson University, Clemson, SC 29634, USA

ARTICLE INFO

Keywords:
Stability constants
Sulfur amino acids
Selenium amino acids
Antioxidants
Copper(II)
Iron(II)

ABSTRACT

Sulfur- and selenium-containing amino acids are of great biological importance, but their metal-binding properties with biologically-relevant metal ions are not well investigated. Stability constants of the methionine, selenomethionine, methylcysteine, and methylselenocysteine with Cu(II) and Fe(II) were determined by potentiometric titration. Stability constants of Cu(II) with these thio- and selenoether amino acids are in the range of 8.0–8.2 ($[CuL]^+$) and 14.5–14.7 (CuL_2) (L = amino acid). Fe(II) interactions with the same thio- and selenoether amino acids are much weaker, with stability constants between 3.5 and 3.8 ($[FeL]^+$) and −4.9 and −5.7 (FeL(OH)). Stability of Fe(II) with penicillamine, a thiol-containing amino acid, is much higher (FeL = 7.48(7) and $[FeL]^{2-}$ = 13.74(2)). For both copper and iron complexes, thio- and selenoether amino acid coordination occurs through the carboxylate and the amine groups as confirmed by infrared spectroscopy, with no stability afforded by thio- or selenoether coordination. The first single-crystal structure of Cu(II) with a selenium-containing amino acid, $Cu(SeMet)_2$, also confirms binding through only the amine and carboxylate groups. The measured Cu(II)-amino-acid stability constants confirm that nearly 100% of the available Cu(II) can be coordinated by these amino acids at pH 7, but very little Fe(II) is bound under these conditions. The relative instability of Fe(II) complexes with thio- and selenoether amino acids is consistent with their inability to prevent metal-mediated oxidative DNA damage. In contrast, the stability constants of these amino acids with Cu(II) weakly correlate to their ability to inhibit DNA damage inhibition.

1. Introduction

Despite the ubiquity and importance of amino acids in biological systems, very little is understood about coordination of labile (non-protein-bound) metal ions by free amino acids. Determining aqueous stability constants for metal ions with biologically relevant ligands, including amino acids, is one way in which more complex systems such as biological fluids or ocean water can be modeled. Fifty years ago, Hallman and coworkers simulated plasma speciation of Cu(II) and Zn(II) with seventeen amino acids [1], but subsequent reviews and analysis of this plasma speciation model revealed deficiencies in the underlying stability constant data since the importance of minor species and redox interactions were neglected [2,3]. More recently, amino acid stability constant data and speciation modeling have been used to help explain copper and zinc deficiencies that occur with total parenteral nutrition [4], trace element speciation in phloem sap [5] and xylem fluid [6], and copper speciation in the eye [7]. More accurate Cu(I) speciation models with penicillamine, cysteine, and glutathione resulted in a better understanding of metallic copper precipitation in the lens and cornea in patients with Wilson's disease [7]. Development of these complex models relies heavily on the accuracy of measured metal-amino-acid stability constants, a particular issue with potentially redox-active sulfur- and selenium-containing amino acids.

Amino acid interactions with copper and iron may also play a crucial role in preventing oxidative damage and diseases that arise due to oxidative stress. Loss of metal homeostasis, mitochondrial malfunction, and the resulting oxidative stress is linked to neurodegenerative disease development, but the mechanistic details that cause this oxidative damage is poorly understood [8–10]. Labile copper and iron produce reactive oxygen species (ROS) such as hydroxyl radical that can damage nucleic acids, proteins, and lipids, and this oxidative damage is catalytic in cells (Fig. 1) [11–13]. Antioxidants capable of disrupting catalytic ROS generation through metal chelation may lessen the oxidative damage leading to Alzheimer's, Parkinson's, Huntington's, and Wilson's

* Corresponding author.
E-mail address: brumagh@clemson.edu (J.L. Brumaghim).

https://doi.org/10.1016/j.jinorgbio.2019.03.001
Received 18 January 2019; Received in revised form 26 February 2019; Accepted 1 March 2019
Available online 04 March 2019
0162-0134/

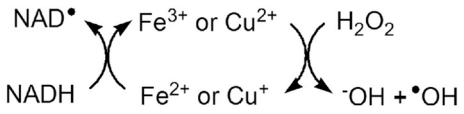

Fig. 1. Catalytic hydroxyl radical generation by iron and copper in cells.

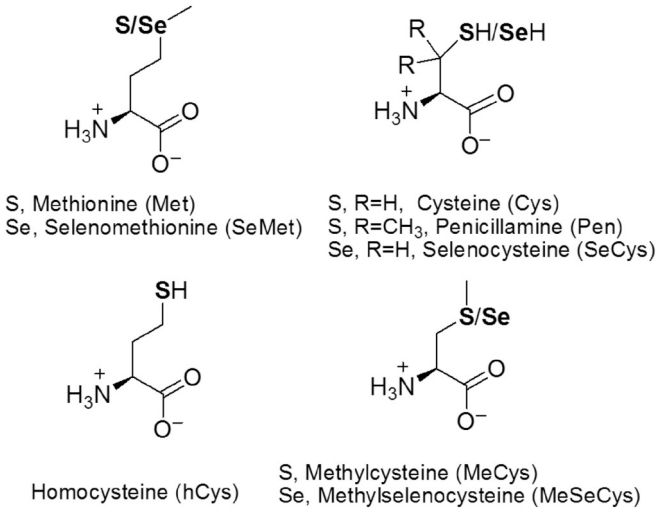

Fig. 2. Structures of common sulfur- and selenium-containing amino acids.

diseases [14]. To ascertain whether amino acid binding to copper and iron may affect their ability to generate ROS, several factors must be determined: the amino acids and other small molecules most likely to interact with labile metal ions, metal ion and amino acid concentrations in the system, and stability constants for the metal-amino-acid complexes.

Naturally occurring and biomimetic sulfur and selenium amino acids with thioether/selenoether and thiol/selenol groups are of significant interest due to their abundance in the active sites of metalloenzymes, their presence in biofluids, and their affinity for binding softer metal ions, such as Cu(I), Cu(II), and Fe(II). A variety of sulfur and selenium amino acids are present naturally (Fig. 2), including methionine (Met), cysteine (Cys), methylcysteine (MeCys), homocysteine (hCys), selenomethionine (SeMet), selenocysteine (SeCys), and methylselenocysteine (MeSeCys). Cys is one of the most prevalent sulfur amino acids [15], with reported concentrations of 256 ± 15 μM in human plasma [16] and 180 ± 20 μM in muscle tissue [17]. Met has somewhat lower concentrations of 69 ± 15 μM [16] and 110 ± 20 μM [17] in plasma and muscle tissue, respectively. Normal levels of hCys in plasma are in the 5–18 μM range [18], and elevated hCys levels are an established risk factor for cardiovascular diseases, cognitive impairment, and chronic renal failure [19–22]. MeCys is not typically used for protein synthesis, but is occasionally incorporated into proteins [23]. MeCys concentrations are not quantified in plasma or cells, but are found at concentrations of 0.2–5 μM in human urine [24]. Although not a natural amino acid, penicillamine (Pen; Fig. 2) is structurally similar to cysteine and is used to chelate and remove excess copper in Wilson's disease [25,26] as well as in the treatment of copper and lead poisoning [27]. When supplemented at 750 mg/day, Pen levels can reach 100 μM in human serum [28].

Biological concentrations of selenium-containing amino acids are not determined, although total selenium concentration in human plasma averages 1.5–1.6 μM with 90% incorporated into selenoproteins as SeCys or SeMet [29]. In humans, total selenium concentration is unlikely to exceed 10 μM due to selenium toxicity [30]. SeCys is the most prevalent selenium amino acid in mammalian selenoproteins [31], but it is difficult to study in solution because its low pK_a (~5) results in dimerization to form the oxidized diselenide species, selenocystine, at physiological pH [32]. In contrast, MeSeCys is the most abundant selenium metabolite in plants [33]. Although selenoamino acids are required for selenoprotein activity [34,35] and can prevent ROS damage [36–38], their interaction with metal ions is not as widely studied as their sulfur-containing analogs.

Many researchers have examined the antioxidant activity of sulfur- and selenium-amino acids [39–44], and Brumaghim et al. [38,45]. established metal binding as a primary antioxidant mechanism for sulfur- and selenium-amino acid prevention of in vitro metal-mediated oxidative DNA damage. Structural analyses and density functional theory determinations established that the HOMO orbital energies of copper-amino-acid complexes predict the observed antioxidant activity [46,47]. However, it is not clear if the stabilities of these amino-acid-metal complexes also correlate with DNA damage prevention ability. Such an analysis is critically hampered by the lack of stability constants for these amino acids with Cu(II) and Fe(II). To test this hypothesis, we determined stability constants for Cu(II) and Fe(II) with sulfur- and selenium-amino acids by potentiometric titration. In addition, metal binding modes of these amino acids with Cu(II) were predicted based on speciation trends, infrared (IR) spectroscopy, mass spectrometry, and solid-state structural determination. We use these measured stability constants and reported metal ion and amino acid concentrations, to discuss the likelihood of metal-amino-acid complex formation in biological systems.

2. Experimental methods

2.1. Materials and instrumentation

Concentrations of stock solutions of copper(II) nitrate trihydrate solutions and iron(II) sulfate heptahydrate were confirmed by inductively coupled plasma-optical emission spectroscopy (ICP-OES). Glycine (Sigma-Aldrich), L-methionine (Alfa Aesar), L-methylcysteine (Sigma-Aldrich), L-selenomethionine (Acros), L-methylselenocysteine (Acros), and D-penicillamine (Alfa Aesar) were purchased from commercial sources. IR spectra were recorded using a Magna 550 IR spectrometer in the range 4000–450 cm^{-1} as Nujol mulls on KBr plates. IR absorption abbreviations are vs, very strong; s, strong; m, medium; w, weak; sh, shoulder.

Electrospray ionization mass spectrometry (ESI-MS) analysis was carried out with a Thermo Scientific (San Jose, CA) TSQ Quantum Access MAX triple quadrupole mass spectrometer. Sample solutions were prepared in 50/50 mixture by volume of CH_3OH/aqueous $NaClO_4$ (10 mM) solution at pH 5. Samples were prepared by mixing Cu(II) or Fe(II) (2 mM) with of the amino acid (4 mM) and introduced to the ESI source by direct infusion. A scan containing 5 micro scans was taken every 0.5 s across a 10 to 1000 Da range. For each sample, 100 scans were collected and averaged to obtain a final spectrum. TSQ Tune software (Thermo Scientific) was used for data acquisition. ESI-MS data are shown in Figs. S4 and S5, and both mass/charge ratios and isotopic distributions match simulated envelope intensities.

2.2. Potentiometric titrations

Titrations were performed using an 836 Titrando equipped with a 800 Dosino autotitrator. A Thermo Sure-flow Ag/AgCl electrode with 0.1 M NaCl filling solution was used to monitor potential of the solution during titration. Amino acid protonation constants were determined by direct titration of 30 mL of a 2.0 mM solution of each amino acid in $NaClO_4$ (0.1 M) to maintain a constant ionic strength. After bubbling with CO_2-scrubbed Ar, the solutions were titrated with CO_2-free, NIST standardized 0.1002 M NaOH using the 836 Titrando equipped with the 800 Dosino to autotitrate.

Cu(II) stability constants with the indicated amino acids were determined using aqueous solutions of $Cu(NO_3)_2{\cdot}3H_2O$ (1.0 mM) and each amino acid (2.0 mM or 3.0 mM) in 1:2 and 1:3 ratios of Cu:ligand and a

constant ionic strength of 0.1 M $NaClO_4$. The electrode was calibrated for the system utilizing NIST-standardized 0.1001 M HCl and 0.1002 M NaOH and the GLEE program [48] to determine standard reduction potentials in 0.1 M $NaClO_4$. For all titrations, 0.1001 M HCl was added to the metal-amino acid solution to bring the solution pH down to 2–3. Copper solutions were bubbled with argon for 15 min and maintained at a constant temperature of 25.0 °C with a jacketed cell under a constant stream of argon to minimize CO_2 contamination of the reaction solutions. The solutions were then titrated as described above for the pure amino acid system. Potentials were measured at 25 °C until precipitation was visible.

Fe(II) stability constants were determined by titrating aqueous solutions of $FeSO_4{\cdot}7H_2O$ (1.0 mM) in 1:2 and 1:3 metal to ligand ratios with solutions of each amino acid (2.0 mM or 3.0 mM) at a constant ionic strength of 0.1 M NaCl in a dry, nitrogen-atmosphere glovebox. All solutions were prepared and titrations were performed in the glovebox. Temperature was maintained at 25.0 °C with a jacketed cell and water circulator. Iron solutions were then titrated with NIST-standardized 0.0100 M NaOH utilizing the 836 Titrando and 800 Dosino autotitrator. Precipitation was observed above pH 8 during iron titrations, except with penicillamine. The iron titrations were back-titrated from pH 10 to 3 to demonstrate reversibility and to improve stability of the electrode over multiple analyses. For all amino acid, Cu(II), and Fe(II) titrations, data were collected in triplicate with reported standard deviations. Potentiometric titration data were analyzed and model-matched using HYPERQUAD2013 [48].

2.3. Synthesis of $Cu(SeMet)_2$

A solution of L-selenomethionine (117.7 mg, 0.6 mmol) in water was added to a solution of $Cu(NO_3)_2{\cdot}3H_2O$ (72.5 mg, 0.3 mmol) in water. NaOH (0.1 M) was added dropwise until the solution reached pH 6.0. The solution was evaporated in air over three weeks, resulting in light-blue crystals as well as powder precipitate. Yield: 106 mg, 78%. IR (cm^{-1}): 3299 w, 3232 w, 3110 s, 1618 vs, 1571 sh, 1462 w, 1340 w, 1304 w, 1138 s, 1083 w, 1246 w, 1160 s, 818 w, 722 w, 671 s, 638 w, 576 s. ESI-MS (*m/z*): 251 $[Cu(C_5H_{11}NO_2Se)]^+$, 274 $[Cu(C_5H_{11}NO_2Se)(OH)]^+$, 456 $[Cu(C_5H_{11}NO_2Se)_2H]^+$. Anal. Calc. for $C_{10}H_{20}CuN_2Se_2O_4$: C, 26.47; H, 4.44; N, 6.17. Found: C, 26.19; H, 4.27; N, 6.01.

2.4. X-ray crystallography

Single crystals for X-ray diffraction were obtained through slow evaporation of a 1:2 metal to ligand solution in water at pH 6, yielding blue, plate-like crystals. A single crystal was mounted on a low background loop and quenched to 100 K in a cold nitrogen stream. Data were collected at this temperature using a Bruker D8 Venture diffractometer with Mo Kα radiation (λ = 0.71073 Å) and a Photon 100 CMOS detector; crystallographic data are summarized in Table S1. A total of 10,345 reflections were collected (3012 independent) using phi and omega scans. Data collection, processing (SAINT), and scaling (SADABS) were performed using the Apex 3 software package [49]. The monoclinic space group $P2_1$ was determined from the systematic absences. The structure was solved using intrinsic phasing (SHELXT) and refined using full matrix least squares techniques (SHELXL) using the SHELXTL software suite [50]. All non-hydrogen atoms were refined anisotropically, and hydrogen atoms were then placed in geometrically optimized positions using appropriate riding models. The presence of two hydrogen atoms on the amine nitrogen atoms was confirmed on the difference electron density map prior to hydrogen atom assignment at these positions. The proper absolute structure was confirmed by a Flack parameter of 0.06(2).

2.5. Plasmid DNA transfection, amplification, and purification

Plasmid DNA (pBSSK) was purified from DH1 *E. coli* competent cells using a ZyppyTM Plasmid Miniprep Kit (400 preps, Fisher). Plasmid was dialyzed against 130 mM NaCl for 24 h at 4 °C to ensure all Tris-EDTA buffer and metal contaminates were removed, and plasmid concentration was determined by UV–vis spectroscopy at a wavelength of 260 nm. Absorbance ratios of $A_{250}/A_{260} \geq 0.95$ and $A_{260}/A_{280} \geq 1.8$ were determined for DNA used in all experiments. Plasmid purity was determined through digestion of plasmid (0.1 pmol) with Sac1 and KpN1 in a 10× Fast Digest Buffer (Thermo Scientific) at 37 °C for 90 min. Digested plasmids were compared to an undigested plasmid sample and a 1 kb molecular weight marker using gel electrophoresis.

2.6. DNA damage gel electrophoresis experiments

For the DNA damage assays with copper, deionized water, MOPS buffer (10 mM, pH 7.0), NaCl (130 mM), ethanol (100%), 10 mM, $CuSO_4{\cdot}5H_2O$, ascorbic acid (7.5 μM, to reduce Cu(II) to Cu(I)), and Pen were combined in an acid-washed (1 M HCl for ~1 h) and dried microcentrifuge tube and allowed to stand for 5 min at room temperature. Plasmid (pBSSK, 0.1 pmol in 130 mmol NaCl) was then added to the reaction mixture and allowed to stand for 5 min at room temperature. H_2O_2 (50 μM) was added and allowed to react at room temperature for 30 min. EDTA (50 μM) was added after 30 min to quench the reaction. For the Fe(II) DNA damage experiments, 2 μM $FeSO_4{\cdot}7H_2O$ and MES buffer (10 mM, pH 6.0) were used. All concentrations are final concentrations in a 10 μM volume. Samples were loaded into a 1% agarose gel in a TAE running buffer; damaged and undamaged plasmid was separated by electrophoresis (140 V for 60 min). Gels were stained using ethidium bromide and imaged using UV light.

Amounts of nicked (damaged) and circular (undamaged) were analyzed using UViProMW software (Jencons Scientific, Inc.). Intensity of circular plasmid was multiplied by 1.24, due to the lower binding affinity of ethidium bromide to supercoiled plasmid [51,52]. Intensities of the nicked and supercoiled DNA bands were normalized for each lane so that % nicked + % supercoiled = 100%. Plots of percent inhibition of DNA damage versus log concentration of amino acid were fit to a variable-slope, sigmoidal dose-response curve using SigmaPlot (v. 9.01, Systat Software, Inc.). IC_{50} value errors represent standard deviations of the values obtained from three separate experiments. Data and IC_{50} plots for all gel electrophoresis experiments are provided in Tables S2–S3 and Figs. S6–S7.

3. Results and discussion

Stability constants measure the thermodynamic likelihood of metal complex formation (Eqs. (1) and (2)) and are directly related to the Gibbs free energy of a system (Eq. (3)). A positive log β indicates favorable thermodynamic stability for complex formation. In this study, potentiometric titrations for multiple metal:ligand molar ratios at 25 °C and pH 3–9 were used to determine stability constants of sulfur and selenium amino acids (L) with Cu(II) and Fe(II) (M), where x is the stoichiometric number of complexing ligands.

$$M + x\,L \rightleftharpoons ML_x \tag{1}$$

$$\beta ML = \frac{[ML_x]}{[M][L]^x} \tag{2}$$

$$\Delta G = -2.30RT\log\beta_{ML} \tag{3}$$

3.1. Amino acid protonation constant determination

Protonation constants for glycine (Gly), Met, SeMet, MeCys, and MeSeCys were determined prior to titrations with metal ions. Although several of these amino acids have established protonation constants, precise determinations of these values under the exact conditions of temperature, ionic strength, and ionic salt used for the Cu(II) and Fe(II)

Table 1
Amino acid protonation constants; amine protonation is represented by K_1 and carboxylate protonation by K_2.

Amino acid	log K_1[a]	log K_2[b]	Temp (°C)	Ionic strength	Reference
Gly	9.67(2)	2.28(5)	25	0.1 M $NaClO_4$	This work
Gly	9.62	2.43	25	0.2 M $NaClO_4$	[53]
Met	9.196(5)	2.09(1)	25	0.1 M $NaClO_4$	This work
Met	9.12	2.22	25	0.2 M KCl	[54]
SeMet	9.29(2)	2.05(1)	25	0.1 M $NaClO_4$	This work
SeMet	9.15	2.37	25	0.1 M $NaNO_3$	[55]
MeCys	8.79(2)	2.02(5)	25	0.1 M $NaClO_4$	This work
MeCys	8.72	2.2	25	0.2 M KCl	[54]
MeSeCys	8.86(2)	2.3(2)	25	0.1 M $NaClO_4$	This work

[a] log K_1 = $[HL]/[H^+][L^-]$.
[b] log K_2 = $[H_2L^+]/[HL][H^+]$.

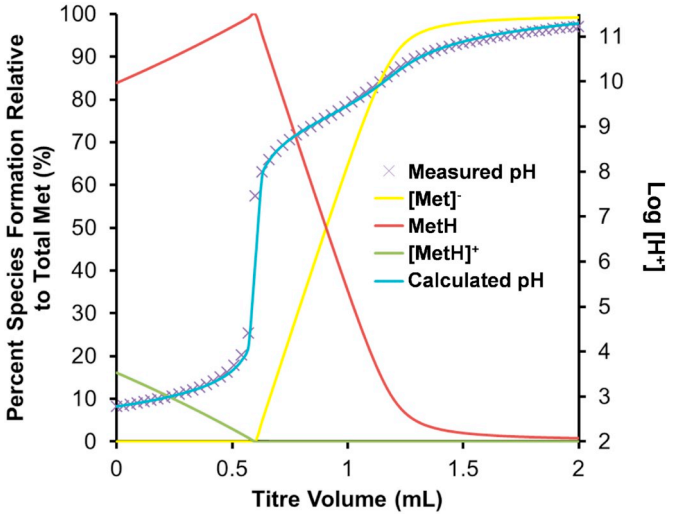

Fig. 3. Representative data and speciation diagrams for the potentiometric titration of the fully protonated amino acids (LH_2, with MeSeCys shown in this example; 0.1 M NaOH, I = 0.1 M $NaClO_4$, 25 °C). The solid blue line represents the modeled titration data with points indicating measured data (pH on the right y-axis); formation of $[MeSeCys]^-$, MeSeCysH, and $[MeSeCysH]^+$ species are indicated as shown in the legend.

titrations were required to ensure consistency and accuracy across all measurements (Table 1). The data agree well with previously reported values, with minor variations due to slightly different analysis conditions, such as differences in the supporting electrolyte. The error is somewhat higher for the pK_2 (< 0.3 log units), which is determined under quite extreme pH conditions. Similarities in the speciation diagrams the thio- and selenoether amino acids and glycine, as represented by the speciation diagram for MeSeCys (Fig. 3), indicate that three separate species (L^-, LH, and LH_2^+) form from pH 3 to 11, with the zwitterionic LH species as the primary species at pH 7. In this zwitterionic form, the amine is fully protonated as an ammonium group (RNH_3^+) and the carboxylic acid is deprotonated as the carboxylate ($RCOO^-$).

Glycine has the highest log K_1 values compared to the thio- and selenoether amino acids, indicating the amine proton is less likely to dissociate. These data represent the first reported protonation constants for methylselenocysteine. Structurally similar MeCys and MeSeCys have the lowest log K_1 values, indicating deprotonation of the ammonium ion to form the amine at lower pH. MeCys and MeSeCys protonation constants are also in close agreement, 8.79(2) and 2.02(5) for log K_1 and 8.86(2) and 2.3(2) for log K_2, respectively, indicating that selenium substitution for sulfur has no significant effect on protonation of the ammonium ion or carboxylic acid. The carboxylic acid dissociation constant (log K_2) is similar for all amino acids (2.02 to 2.3), and thus exists as the carboxylate ion at biologically relevant pH values.

3.2. Cu(II)-amino acid stability constants

Cu(II) stability constants with the sulfur-containing amino acids have been widely studied [1,3,4,54,56–67] due to their bioavailability and their role in metal coordination in metalloproteins. Two species are identified, $[CuL]^+$ and CuL_2, where L^- represents the amino acid with amine and carboxylate groups. For Met, SeMet, MeCys, and MeSeCys, the S/Se atom in the side chain can potentially bind Cu(II) in addition to the amine N and carboxylate O atoms, resulting in a tridentate species. Such tridentate binding occurs for Cu(II)-amino-acid complexes such as $Cu(His)_2$ (His = L-histidine) [68], and $[Cu(Asp)(phen)(H_2O)]$ (Asp = aspartic acid; phen = 1,10-phenanthroline) [69]. Glycine is well known to bind Cu(II) in a bidentate fashion [70] but cannot bind through the side chain to become a tridentate chelator; therefore, it was included in this study as a bidentate-binding control. If the thio- or selenoether S/Se atom participates in tridentate binding to Cu(II), higher stability constants are expected compared to those of the Cu(II)-Gly system.

Cu(II) stability constants were determined for Gly, Met, SeMet, MeCys, and MeSeCys at 25 °C with a constant ionic strength of 0.1 M $NaClO_4$ to provide a self-consistent data set. Titrations were performed in triplicate at metal-to-ligand ratios of 1:2 and 1:5, and stability constants describing metal-ligand binding are provided in Table 2. For all the Cu(II) titrations, precipitation occurred above pH 8, except for the Cu(II)-SeMet system in which precipitation began at pH 5. A representative speciation graph for the Cu(II)-MeSeCys titrations at a 1:2 Cu:amino acid ratio is provided in Fig. 4.

Only two species are present at pH 7, $[Cu(MeSeCys)]^+$ and $Cu(MeSeCys)_2$ (Fig. 4), and the $Cu(MeSeCys)_2$ species reaches a maximum concentration around pH 8, approximately the pH that precipitation occurs. This speciation is consistent with all of the ligands studied with Cu(II), although precipitation occurs at pH 5 with SeMet due to the insolubility of the complex. When the full data set (pH 2–10) was included in the modeling, incorporation of a third species, Cu(L)(OH), resulted in a better fit. A direct comparison of the two models is provided in Figs. S1 and S2 for the Cu-Met system. Ultimately, the Cu(L)(OH) species was excluded from the analysis because its log β value was extremely low. Since this putative Cu(L)(OH) species forms at pH 8 and above, it is more likely that deviation in the fit reflects the instability of the system as Cu(II) and L^- are depleted due to precipitation, rather than the presence of a new species. The precipitate was confirmed as $Cu(MeSeCys)_2$ by IR analysis (see Proof of speciation for Cu(II) complexes section). All the thio- and selenoether amino acids as well as glycine form the same $[CuL]^+$ and CuL_2 species.

3.3. Proof of speciation for Cu(II) complexes

Speciation in the Cu(II)-thio- and selenoether amino acid systems was confirmed using a variety of solution and solid-state analyses. For the soluble Cu(II)-Met species, electrospray ionization mass spectrometry (ESI-MS) confirmed the presence of $[Cu(Met)]^+$ (212 m/z; Fig. S4). The Cu(Met)(OH) (230 m/z) species was also identified; however, the samples were prepared at pH 5, well below the pH where modeling indicates possible formation of this species. Thus, this species most likely arises from water coordination of the $[Cu(Met)]^+$ species. Since Gly, Met, SeMet, MeCys, and MeSeCys all have Cu(II) stability constants within 0.5 log units, the resulting species are assumed to bind Cu(II) similarly.

Above pH 8, the Cu(II)-amino-acid complexes precipitated, and IR spectroscopy was used to confirm CuL_2 formation of the species and to compare with reported spectra (Table 3) [55,79–81]. For $Cu(Met)_2$ and $Cu(SeMet)_2$, broad N–H stretching absorption bands at 3077 and 3080 cm^{-1} for Met and SeMet, respectively, split into three distinct stretching vibrations for the corresponding Cu(II) complexes: 3300,

Table 2
Stability constants for Cu(II)-amino acid complexes determined by potentiometric titration.

Amino acid	ML (log β)[a]	ML_2 (log β_2)[b]	ML(OH) (log β_{-1})[c]	Temp (°C)	Ionic strength (M)	Reference
Cu(II) stability constants						
Gly	8.11	14.96		25	0.1	[71]
	8.26(1)	15.10(5)		25	0.1 $NaClO_4$	This work
Met	7.85(2)	14.52(1)		25	0.1 KNO_3	[60,62,72]
	7.96(5)	14.65(7)		25	0.1 $NaClO_4$	This work
MeCys	7.65[d]	14.13[d]		25	0.2 KCl	[73]
	8.05(5)	14.47(5)		25	0.1 $NaClO_4$	This work
SeMet	7.77[d]	14.50[d]		25	0.1 $NaNO_3$	[55]
	8.02(2)	14.63(2)		25	0.1 $NaClO_4$	This work
MeSeCys	8.2(1)	14.5(2)		25	0.1 $NaClO_4$	This work
hCys	11.92(1)	13.54(2)[e]	7.57(1)	25	0.1 KNO_3	[74]
Pen	16.5[d]	21.7[d]		25	0.15 KNO_3	[75]
Fe(II) stability constants						
Gly	4.13[d]	7.65[d]		25	0.1 KNO_3	[76]
	4.04(5)		−4.24(2)	25	0.1 $NaClO_4$	This work
Met	3.24[d]			20	1.0 KCl	[77]
	3.51(3)		−4.9(1)	25	0.1 $NaClO_4$	This work
MeCys	3.49(4)		−5.7(1)	25	0.1 $NaClO_4$	This work
SeMet	3.51(7)		−5.3(3)	25	0.1 $NaClO_4$	This work
MeSeCys	3.84(1)		−5.08(2)	25	0.1 $NaClO_4$	This work
Cys	6.69(2)	11.90(3)		20	0.1 $NaClO_4$	[78]
Pen	7.58(1)	13.74(2)		20	0.1 $NaClO_4$	[78]
	7.48(7)	13.91(7)		25	0.1 $NaClO_4$	This work

[a] $\log \beta = [M][L]/[ML]$.
[b] $\log \beta_2 = [M][L\text{-}]^2/[ML\text{-}_2]$.
[c] $\log \beta_{-1} = [ML][OH]/[ML(OH)]$.
[d] No error reported.
[e] Reported as the [MHL] species, not the [ML_2] species.

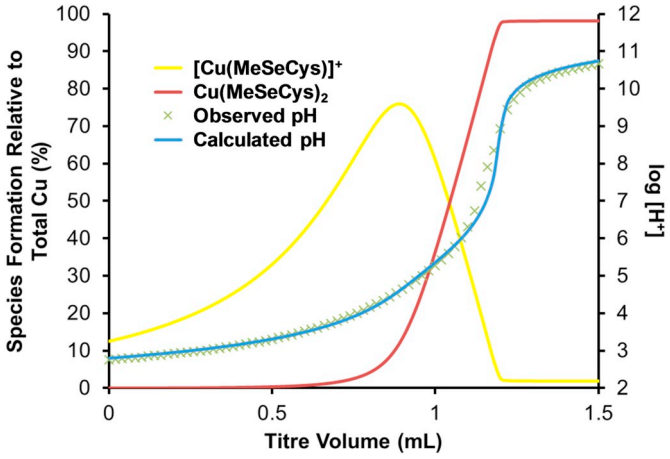

Fig. 4. Representative titration and speciation diagram for the potentiometric titration of Cu(II) and methylselenocysteine (MeSeCys) in a 1:2 ratio (0.1 M NaOH, I = 0.1 M $NaClO_4$, 25 °C). The solid blue line represents the modeled titration and points represent the measured data. Formation of [Cu(MeSeCys)]$^+$ and $Cu(MeSeCys)_2$ species are indicated as shown in the legend.

3241, and 3120 cm^{-1} for the Met complex and 3281, 3233, and 3132 cm^{-1} for the SeMet analog. This N—H splitting confirms participation of the amine nitrogen in Cu(II) binding, since the environment of the amine protons change slightly to compensate for the loss of freedom due to the proximity of the copper ion [55]. Amine binding is further supported by a N—H deformation band that appears at 1569 cm^{-1} for Met and 1570 cm^{-1} for SeMet. Carboxylate oxygen binding is also indicated by the shift of the asymmetric C—O stretch from approximately 1610 cm^{-1} to 1622 and 1616 cm^{-1} for the Met and SeMet complexes, respectively [55,80]. M—N and/or M—O bond formation is also indicated by the presence of one or two absorbances in the 440–600 cm^{-1} region [79].

IR results for MeCys and MeSeCys are consistent with the trends observed with the aforementioned Met and SeMet, although the C=O stretch observed at approximately 1620 cm^{-1} for the other complexes was shifted to 1640 cm^{-1} for the MeSeCys and no discernible NH_2 deformation was observed. Trends observed in the IR spectrum of Cu(MeSeCys)$_2$ can help confirm that the same structural confirmations are being formed in the binding of the [MeSeCys]$^-$ ligand to the Cu(II) as has been shown with the other thio- and selenoether amino acids. The stability constants indicate similar coordination for all of the thio- and seleno-ether amino acids.

Table 3
IR data for metal-amino-acid complex precipitates in potentiometric titrations (pH > 8; NR = not reported).

Vibration	$Cu(Met)_2$[a] (cm^{-1})	$Cu(Met)_2$ (cm^{-1})	$Cu(MeCys)_2$[b] (cm^{-1})	$Cu(MeCys)_2$ (cm^{-1})	$Cu(SeMet)_2$ (cm^{-1})	$Cu(MeSeCys)_2$ (cm^{-1})	$Fe(Met)_2$ (cm^{-1})
NH_2 stretching	3390	3300	3300	3299	3281	3322	3410
	3230	3241	3230	3232	3233	3221	3360
	3130	3120	2990	3110	3132	3130	3289
C=O stretch	1620	1622	1620	1618	1616	1640	1598
NH_2 deformation	1580	1569	1570	1571	1570	1571	1562
C—N vibration	NR	1337	NR	1340	1399	1335	1330
M—N and/or M—O stretch	NR	578	NR	576	497	521	568

[a] From reference [79].
[b] From reference [80].

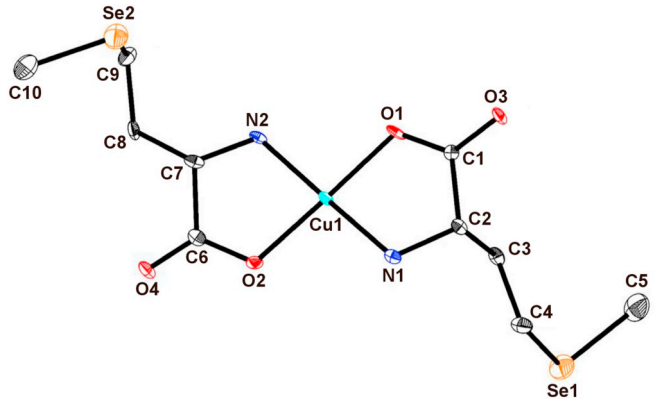

Fig. 5. Structure of $Cu(SeMet)_2$ shown with 70% probability ellipsoids for $Cu(SeMet)_2$. Hydrogen atoms are omitted for clarity.

Table 4
Selected bond lengths (Å) and angles (°) for $Cu(SeMet)_2$.

	Bond lengths (Å)		Angles (°)
Cu1-N1	1.992(6)	O2-Cu1-O1	178.3(2)
Cu1-N2	1.980(6)	O2-Cu1-N2	84.4(2)
Cu1-O1	1.954(5)	O1-Cu1-N2	94.8(2)
Cu1-O2	1.950(5)	O2-Cu1-N1	96.2(2)
Cu1-O4[a]	2.640(4)	O1-Cu1-N1	84.4(2)
Cu1-O3[a]	2.687(4)	N2-Cu1-N1	175.5(2)
C4-Se1	1.952(7)	C4-Se1-C5	98.4(3)
C5-Se1	1.953(9)	C10-Se2-C9	98.5(4)
C9-Se2	1.958(7)		
C10-Se2	1.939(9)		

[a] Cu1-O3 and Cu1-O4 represent the carboxylate-bridged, apical bond distances in the packing diagram (Fig. S3).

Amine nitrogen and carboxylate oxygen coordination to Cu(II) is strongly supported by the solid-state structure of $Cu(SeMet)_2$ (Fig. 5 and Table 4), the first structure for a Cu(II)-seleno amino acid complex. In $Cu(SeMet)_2$, each SeMet ligand coordinates copper through bidentate binding of nitrogen and oxygen atoms in the equatorial position, resulting in an overall distorted square planar geometry ($\tau_4 = 0.043$) around Cu(II) (Cu—N = 1.980(6) and 1.992(6) Å; Cu—O = 1.950(5) and 1.954(5) Å). This is similar to the thioether complexes $Cu(Met)_2$ (Cu—N = 1.97(1) and 2.01(1) Å; Cu—O = 1.944(8) and 1.970(8) Å) [79,82] and $Cu(MeCys)_2$ (Cu—N = 1.994 and 2.000 Å; Cu—O = 1.936(1) and 1.951(1) Å) [80]. All other bond lengths and angles are comparable to those in the $Cu(Met)_2$ structure reported by Ou and coworkers [79], with the exception of a slight lengthening in the carbon-chalcogen bonds, averaging 1.950(9) for the C—Se bonds in the present study compared to 1.80(2) Å for the C—S bonds in $Cu(Met)_2$. This lengthening may result in the slightly longer *c*-axis of the selenoether complex (16.082(1) Å) compared to the thioether complex (15.563(8) Å).

Carboxylate oxygen atoms from neighboring molecules form axial bonds to the Cu centers with extended copper-oxygen bond lengths of 2.640(4) and 2.687(4) Å, significantly longer than the equatorial carbon-oxygen bonds of 1.950(5) and 1.954(5) Å. These apical interactions result in the formation of sheets in the *ab*-plane (Fig. S3). Hydrophobic intermolecular interactions of the Se-CH_3 side chains isolate neighboring sheets from one another along the *c*-axis. The structures of $Cu(Met)_2$ and $Cu(MeCys)_2$ also crystallize in space group $P2_1$ and feature similar long range motifs directed by the axial interactions of Cu(II) with carboxylate groups, although in the case of $Cu(MeCys)_2$, the sheets occur in the *bc*-plane, and the β angle is expanded somewhat to 97.55(2)° [79,80,82].

Similar elongated Cu-carboxylate axial interactions are observed in Cu(II)-glycine-based structures [83,84]; however, some Cu(II)-glycine structures instead incorporate one [85–88] or two [70] water molecules in the axial positions. This water coordination in the solid state suggests that Cu(II) would likely be hydrated in solution, especially for $[Cu(Met)]^+$ and similar amino acid species with open coordination sites around the central metal ion. Water coordination at pH < 7 also suggests formation of species with hydroxide ligands at pH > 7, although these species may not be readily identifiable in titrations due to complex precipitation.

3.4. Structure-stability analysis for Cu(II)

Cu(II)-MeSeCys stability constants are reported for the first time as 8.2(1) and 14.5(2) for the $[Cu(MeSeCys)]^+$ and $Cu(MeSeCys)_2$ species, respectively (Table 2). The higher error for these MeSeCys titrations relative to other thio- and selenoether amino acid values is likely due to interactions of the soft selenoether species with the electrode. To mitigate this issue, MeSeCys titrations were back-titrated to demonstrate reversibility. Without the back-titration, the electrode response degraded with subsequent trials. Cu(II)-MeSeCys stability constants are within 0.5 log units of those for the other thioether and selenoether amino acids, suggesting similar binding modes.

Stability constants of Cu(II) with Met, SeMet, and MeCys are within 0.2 log units for the $[ML]^+$ species (7.96(5) to 8.05(5) and ML_2 species (14.47(5) to 14.65(7)), although they are slightly higher than reported results (Table 2). The lack of variation in these values indicates that there is little difference in Gly, Met, MeCys, and SeMet thermodynamic stability upon Cu(II) binding. Small variations in these values are likely due to differences in supporting electrolyte or in time allowed for the titrations to reach equilibrium.

For analogous sulfur and selenium amino acids, such as Met/SeMet and MeCys/MeSeCys, our data suggest that Cu(II) coordination to the selenoether moiety may be slightly more stable than coordination to the thioether moiety, but the differences in stability constants for the $[CuL]^+$ species (0.06 between SeMet and Met and 0.1 between MeCys and MeSeCys) are almost within the measured uncertainty. A small increase in stability may also be observed for $[CuL]^+$ species of amino acids with shorter side chains (MeCys vs. Met and MeSeCys vs. SeMet), although these differences are also quite small (0.09 between MeCys and Met and 0.2 between MeSeCys and SeMet).

A comparison of the data for the CuL_2 species indicates no differences in stability due to substitution of selenium for sulfur, but the longer side chains of Met (14.65(5)) and SeMet (14.63(2)) formed slightly more stable complexes as opposed to MeCys (14.47(5)) and MeSeCys (14.5(1)). The greater relative stability of Cu(II) binding to Gly compared to thioether and selenoether amino acids corroborates our solid-state results that show no Cu(II)-S/Se binding, and in fact that thio- and selenoether side chains slightly destabilize these complexes in solution.

Under certain conditions, Cu(II) complexes of thiol-containing amino acids are more stable than their thio- and selenoether counterparts (Table 2), however, the redox interaction of Cu(II) with thiols makes speciation determination extremely difficult. In contrast to the thio- and selenoether functional groups, thiols have ionizable protons and thiol-containing amino acids have four possible protonation states: $[H_3L]^+$, $[H_2L]$, $[HL]^-$, and L^{2-}. The tendency of cysteine and penicillamine to reduce Cu(II) and Cu(I) has been previously examined [89,90], and the products formed are highly dependent on metal:ligand ratio and the supporting electrolyte. Gergely and coworkers report three different scenarios for Cu(II)-Pen titrations: (1) when the ligand:metal ratio is > 2, a Cu(I)-Pen with polymeric structure is obtained, (2) when the ligand:metal ratio is between 1 and 2 and a halide (Cl, Br, or I) is present, a mixed-valence cluster is obtained, and (3) when the ligand:metal ratio is between 1 and 2 and a different ion is available (nitrate, fluoride, thiocyanate, sulfate), a blue solution that is similar in UV absorbtivity to Cu(II)-thioether complexes is obtained. In potentiometric titrations with Cu(II), both hCys and Pen form CuL

species (Table 2) [74,75], and Rosen and Kuchinkas [75] also identified a $[Cu(Pen)_2]^{2-}$ species. To date, no selenol-copper stability constants have been reported, likely due to the low pK_a of selenols (~5) and the resulting tendency to form diselenide species [32].

Other reported Cu(II) complexes of thiol-containing amino acids are not consistent: Pinto and coworkers [74] identified $[Cu(HhCys)]^+$ and [Cu(hCys)(OH)] species in a potentiometric titration of a 1:1 Cu(II) to hCys (to prevent Cu(II) oxidation of hCys) and identified $Cu(hCys)_2$ as a precipitate at higher ligand-to-metal ratios. Based on our model simulations using the stability constant values reported by Pinto et al. [74], the Cu(hCys)(OH) species is the dominant species above pH 4, with no evidence for formation of the $[Cu(HhCys)]^+$ species under the given experimental conditions. Solid-state analysis of $Cu(hCys)_2$ by IR and EPR spectroscopy indicated bidentate Cu(II) coordination of the amine and thiolate groups, with no binding through the carboxylate group.

In contrast, tridentate Cu(II) coordination in the solid state is reported for Pen, and in a unique polymeric structure supported by a gold-bis(diphenylphosphino)alkane linker, Cu(II) coordinates two Pen ligands, one in a tridentate fashion through the amine, carboxylate, and thiolate groups, and one in a bidentate fashion through only the amine and thiolate [91]. Higher stability constants for the thiol-containing amino acids with Cu(II) indicate increased stability compared to thioether and selenoether amino acids and Gly, either due to increased stability of an amine and side-chain thiolate coordination or tridentate chelation of the copper by the carboxylate, amine, and thiolate groups, when copper redox reactions can be controlled.

3.5. Fe(II)-amino acid stability constants

Even though iron is the most abundant transition metal ion in biological systems, stability constant data for Fe(II) with sulfur and selenium amino acids is much more limited than for Cu(II). Since Fe(II) is more difficult to work with due to its tendency to oxidize in air, titrations must be performed under nitrogen or argon to exclude oxygen during analysis. In addition to oxygen sensitivity, Fe(II)-amino acid complexes precipitate above pH ~8, limiting the analysis window for potentiometric titrations. Likely because of these limitations, Met is the only thio- or selenoether amino acid with reported Fe(II) stability constants [56,92], and data from these 1950s papers are inconsistent. Perrin [92] reports a stability constant of 3.42 for a $[Fe(Met)]^+$ species; however, Albert [56] reports formation of a $Fe(Met)_2$ species with a stability constant of 6.7. In neither study were the identified species investigated using alternative methods.

To address the paucity of Fe(II) stability constant data with sulfur and selenium amino acids, potentiometric titrations of Fe(II) with Met, MeCys, SeMet, MeSeCys, and Pen at a 1:2 and 1:3 metal to ligand ratio were performed in a nitrogen-atmosphere glovebox. Similar to the Cu (II) studies, glycine titrations with Fe(II) were performed for comparison. Because precipitation is observed above pH 8, with the exception of the Fe(II)-Pen system that shows no precipitation up to pH 10, titrations were restricted to a maximum of pH 8. These titrations indicate formation of $[FeL]^+$ and FeL(OH) complexes with Gly, Met, SeMet, MeCys, and MeSeCys (Fig. 6A and Table 2). In contrast, Fe(II) titrations with thiol-containing Pen indicate formation of Fe(Pen) and $[Fe(Pen)_2]^{2-}$ species (Fig. 6B) in excellent agreement with previous analyses [78].

Stability constants for the 1:1 $[Fe(Gly)]^+$ and $[Fe(Met)]^+$ agree with previously reported data (Table 2) [76,77,92–94]. For Gly titrations, Gergely [76] also identifies a $Fe(Gly)_2$ species with a log β of 7.65, whereas Micskei [94] identifies two additional species, $Fe(Gly)_2$ with a log β of 6.65(1) and $[Fe(Gly)_3]^-$ with a log β of 8.87(1). Under our titration conditions, these $Fe(Gly)_2$and $[Fe(Gly)_3]^-$ species are not present; instead, a Fe(Gly)(OH) species is observed with a stability constant of −4.24(2). In Met titrations, a similar Fe(Met)(OH) species is also identified, but the $Fe(Met)_2$ species reported by Albert [56] is not. Due to a lack of reported detail, it is unclear how these titrations differ

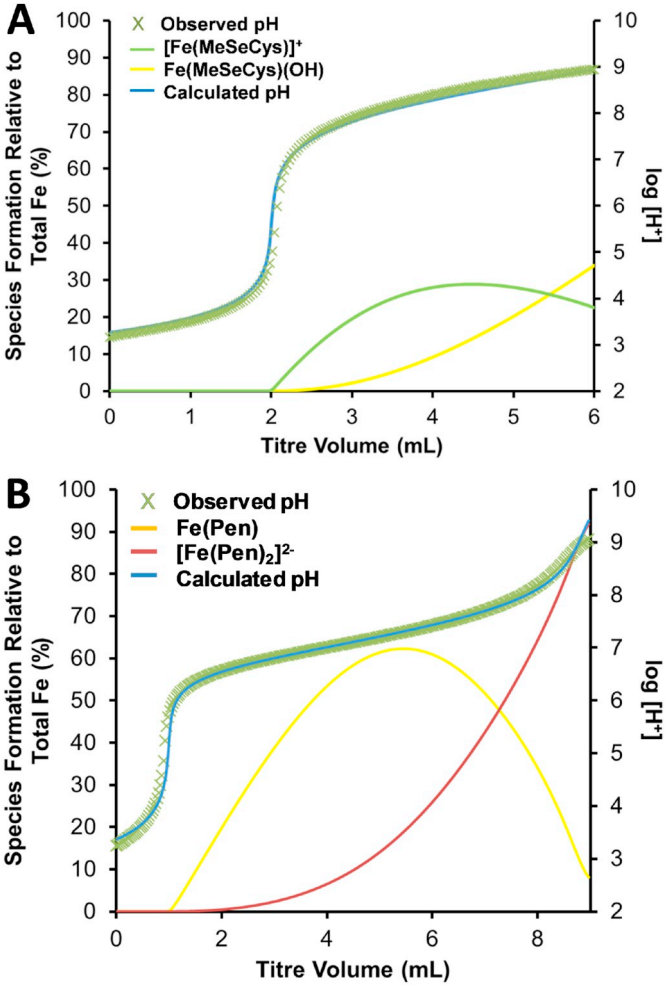

Fig. 6. Representative titrations (0.01 M NaOH, I = 0.1 M NaCl, 25 °C) and speciation diagrams for the titration of A) Fe(II) and methylselenocysteine in a 1:2 ratio and B) Fe(II) and penicillamine in a 1:2 ratio. The solid blue line represents the modeled titration, and points represent the measured data. Formation of Fe(II)-amino-acid species are indicated as shown in the legend.

from the analysis by Albert, although the authors of these studies included data above the pH at which precipitation begins to occur, perhaps skewing the fit of their models.

Stability constants for the 1:1 species of Fe(II) with MeCys, SeMet, and MeSeCys were determined to be 3.49(4), 3.51(7), and 3.84(1), respectively (Table 2), representing the first stability constant determinations for Fe(II) with these amino acids. These $[FeL]^+$ stability constants are similar to those for $[Fe(Gly)]^+$ (3.73(1)) and $[Fe(Met)]^+$ (4.13) [76,77]. As noted for the Cu(II) titrations, the $[Fe(Gly)]^+$ stability constant is slightly higher than those for any of the thio- or selenoether amino acids, likely indicating no Fe(II)-S/Se binding. In contrast to previous reports, presence of the FeL(OH) species (L = Met, SeMet, MeCys, MeSeCys) is identified in the best fit model for these systems, with this species growing in above pH 4 as hydroxide becomes more readily available.

For Fe(II) titrations with the thiol-containing Pen, our data are consistent with formation of [Fe(Pen)] and $[Fe(Pen)_2]^{2-}$ species, with stability constants of 7.48(7) and 13.91(7), respectively. These results closely match those reported by Doornbos [78] in 1964 (Table 2), although formation of polymeric species cannot be ruled out. The lack of precipitation in this system up to pH 10 is likely due to strong Fe(II)-thiolate interactions as well as the greater charge of $[Fe(Pen)_2]^{2-}$ that makes it more soluble in aqueous solution than the $[FeL]^+$ species formed by the thio- and selenoether amino acids. These speciation

differences in the Fe(II)-Pen and Fe(II)-MeSeCys systems are obvious when comparing their respective titration data (Fig. 6). In fact, Fe(II)-Pen complexes are slightly more stable than Fe(II)-Cys complexes based on comparisons with reported data (Table 2).

3.6. Proof of speciation for Fe(II) complexes

Proof of speciation using mass spectrometry was more difficult for the representative Fe(II)-Met system than for the analogous Cu(II)-Met system, likely due to the weaker stability constants determined for the Fe(II) species. By ESI-MS only the Fe(III) species, $[Fe(Met)_2]^+$ (m/z = 353; Fig. S5), is observed due to Fe(II) oxidation during injection and ionization. Precipitate formed during Fe(II)-Met titrations was analyzed using IR spectroscopy to determine amino acid binding modes as a representative sample of the Fe(II)-thioether and -selenoether interactions. As discussed in detail for the Cu(II)-amino acid complexes, shifts in both the N−H and C═O stretches for $Fe(Met)_2$ (Table 3) compared to unbound Met indicate Fe(II) coordination through both the amine nitrogen and the carboxylate oxygen atoms, similar to the IR spectrum of the fully characterized $Cu(Met)_2$. In addition, the absence of a broad absorption in the 3500–3700 cm^{-1} range indicates that no hydroxide or water is coordinated. The Fe(II)-Pen species were not confirmed by IR, because they do not precipitate in aqueous solution. As discussed by Doornbos and Faber [78], formation of the Fe(II) complex as the thiol deprotonates is consistent with coordination through the amine and thiolate groups.

The only single crystal structure for Fe(II) with any amino acid is $Fe(Pro)_2(phen)$ (Pro = L-proline; phen = 1,10-phenanthroline [95]), which binds Fe(II) through the amine N and carboxylate O atoms. The only stability constant reported for the Fe(II)-Pro system is for the ML_2 complex (log β = 8.3), determined by Albert [56] in 1950. This low stability constant indicates extremely weak Fe(II) coordination, similar to those observed for the thio- and selenoethers, but does indicate that bidentate binding of thio- and selenoether amino acids is likely. Since all of the FeL_2 stability constants with the thio- and selenoether amino acids were similarly low and approximately the same as the $Fe(Pro)_2$ stability constant, it is reasonable to assume that the coordination environments are similar. The lack of reported solid-state structures for Fe(II)-amino-acid complexes is indicative of this weak coordination and difficulty in working with oxygen-sensitive Fe(II) complexes.

3.7. Structure-stability analysis for Fe(II)

Fe(II)-amino acid stability constants for the $[FeL]^+$ species with the thio- and selenoether amino acids are within 0.5 pH units of each other (3.49(4) to 3.84(1); Table 2), and stability constants for the FeL(OH) complexes are in the range −4.9(1) to −5.7(1), slightly less accurate due to precipitation at pH 8. The $[Fe(Gly)]^+$ stability constant is slightly higher (4.04(5)) than those of the thio- and selenoether amino acids, indicating that the sulfur and selenium atoms of these amino acids do not contribute to complex stability.

In contrast, the thiol-containing Pen exhibits stronger binding to Fe(II), with Fe(Pen) and $[Fe(Pen)_2]^{2-}$ stability constants of 7.48(7) and 13.91(7), respectively, similar to Cu(II) stability constants with the thio- and selenoether amino acids, but much higher than the stability constant for $[Fe(Gly)]^+$ (Table 2). Similarities in the stability constants for the Fe(II)-Pen and Cu(II)-Met systems suggest bidentate coordination, although Pen likely binds through the thiolate sulfur, replacing either the amine nitrogen or the carboxylate oxygen. Stability constants for Cu(II) with penicillamine have been reported as 16.5 and 21.7 for the Cu(Pen) and $[Cu(Pen)_2]^{2-}$ species, respectively (Table 2). This significant increase in stability compared to Fe(II)-Pen complexes strongly suggests tridentate Cu(II) coordination of the thiolate, amine, and carboxylate groups, a trait critical for its use as a biological Cu(II) chelator to treat Wilson's disease.

Greater binding stability for Cu(II) over Fe(II) coordination was determined for all the sulfur and selenium amino acids in Table 2. Stability constants of approximately 8 for the $[CuL]^+$ species and approximately 4 for the $[FeL]^+$ species, indicate a much lower affinity of the amino acid for Fe(II) in comparison to Cu(II). This may be due to differences in electronic environment and/or preferred coordination geometries around these two divalent metal ions. The extremely low $[FeL]^+$ stability constants indicate unlikely complex formation in a competitive environment of other biomolecules with much higher stability constants.

3.8. Cu(II)/Fe(II) competition for sulfur- and selenium-containing amino acid binding at biological concentrations

Iron is the most abundant transition metal ion in biological systems, with labile pools as high as 10 μM in human lymphocytes [96]. Copper is the third-most abundant transition metal, and although labile copper concentrations have not been determined [97,98], total copper levels are as high as 100 μM in brain tissue [99]. Stability constants of Cu(II) with thio- and selenoether amino acids are in the range of 8.0–8.2 for $[CuL]^+$ species; however Fe(II) interactions with the same thio- and selenoether amino acids are much weaker, with stability constants between 3.5 and 3.8 for analogous $[FeL]^+$ species. Similarly, the ML stability constant for Cu(II) with Pen is significantly higher than that reported for Fe(II) (16.5 and 7.6, respectively; Table 2). Despite much weaker Fe(II) coordination compared to Cu(II), higher labile Fe(II) concentrations may allow it to compete with Cu(II) for binding to available amino acids.

To investigate this possible competition, we modeled a system incorporating Cu(II) (1 μM), Fe(II) (10 μM), and the strongest-binding amino acid, Pen (1–100 μM), at pH 7. These concentrations were chosen based on approximate labile concentrations for iron [96] and reported concentrations for Pen in patients being treated for Wilson's disease [28]. Although exact labile concentrations for Cu(II) are not reported [97,98], a 1 μM concentration was chosen to examine the effect of a ten-fold difference between copper and iron levels.

Under these conditions, formation of the Cu(Pen) species is unaffected by the availability of excess Fe(II) (Fig. S8). At the lowest concentrations, Pen is initially equimolar to Cu(II) and ten times less concentrated than Fe(II). At these ratios, 99.8% of the Cu(II) (0.998 μM) is coordinated to penicillamine. As the Pen concentration rises, only limited Fe(II) coordination is observed, even when Pen is ten times more concentrated than Fe(II). A maximum of 3.9% of the Fe(II) (0.393 μM) is coordinated by Pen in this simulation. The $[Cu(Pen)_2]^{2-}$ and $[Fe(Pen)_2]^{2-}$ species are only observed in trace amounts (< 0.1 μM) and are not contributing species in this model. Since limited coordination of labile Fe(II) is observed even at a 10-fold excess of Pen, a 10-fold excess of available Fe(II) does not outcompete Cu(II)-Pen complexation.

3.9. Correlation of stability constants with amino acid antioxidant ability and biological speciation

Iron- and copper-mediated DNA damage can lead to oxidative stress and cell death, and sulfur and selenium compounds have been widely examined for their ability to inhibit DNA damage by Fe(II) or Cu(II)-mediated hydroxyl radical generation (Fig. 1). In vitro gel electrophoresis studies quantified the concentration of thio- and selenoether amino acids required to inhibit 50% of the DNA damage (IC_{50} values) caused by Fe(II) or Cu(I) and hydrogen peroxide (Table 5). Brumaghim and coworkers [38,45,100] established that this antioxidant behavior was due to metal-amino-acid coordination, although they did not attempt to correlate DNA damage prevention with stability constants.

To investigate potential correlations between metal-amino-acid binding and DNA damage prevention, we examined the relationship between the IC_{50} data (Table 5) and stability constants for the $[CuL]^+$ and CuL_2 species with Gly, Met, SeMet, MeCys, and MeSeCys. Data for

Table 5
Inhibitory concentrations for metal-mediated DNA damage prevention by amino acids.

Amino acid	Cu(I) IC_{50} (μM)	Fe(II) IC_{50} (μM)	Reference
Gly	22.4 ± 0.1	None	[101]
Met	11.8 ± 1.3	None	[45]
SeMet	25.1 ± 0.1	None	[38]
MeCys	9.6 ± 1.0	None	[45]
MeSeCys	8.64 ± 0.02	None	[38]
Pen	26.9 ± 0.1	591 ± 1	This work[a]

[a] Data and IC_{50} plots for DNA damage prevention experiments with Pen are provided in Tables S2–S3 and Figs. S6–S7.

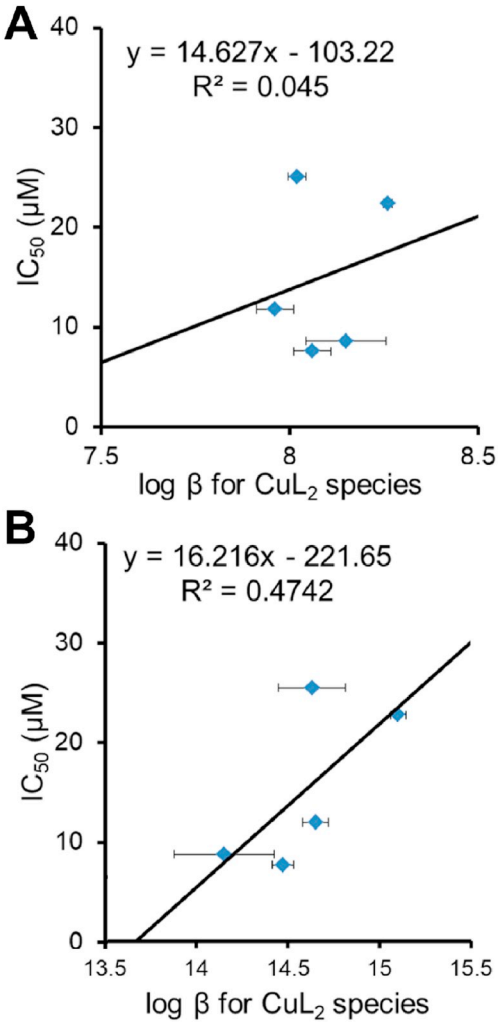

Fig. 7. Graphs of A) stability constants of the CuL species and B) stability constants of the CuL_2 species vs. 50% inhibitory concentrations for oxidative DNA damage (IC_{50} values) for the amino acid antioxidants (L) in Table 5. Solid lines show the best-fit trend line for the data with the equations given.

the Cu(II)-Pen system were excluded from this analysis due to the differences in metal binding modes. Although stability of the ML species and inhibition of metal-mediated DNA damage are not correlated (R^2 = 0.045; Fig. 7A), a weak correlation exists between stability constants for the ML_2 species and DNA damage prevention (R^2 = 0.4742; Fig. 7B). This limited correlation indicates that the stronger the Cu(II)-amino-acid binding, the less effective the amino acid is at preventing metal-mediated DNA damage.

These DNA damage inhibition assays use Cu(I)/H_2O_2 to generate damaging hydroxyl radical, and Cu(I) complexes are not expected to have the same stability constants as Cu(II). A comparison of Cu(I) stability constants with IC_{50} values would be ideal, but only Cu(I) stability constants with Cys [7], Pen [7], and Met [77] are reported, due to the difficulty of working with Cu(I) in aqueous systems. Cu^{I}(Met) has a higher log β than $[Cu^{II}(Met)]^+$ species (9.1 vs. 7.65, respectively [77]) so Met is more stable binding Cu(I) than Cu(II), but data are too limited to establish trends.

Perhaps the most relevant general trend of complex stability with DNA damage prevention can be elucidated from the poor stability of the Fe(II)-thioether and -selenoether complexes. Thio-and selenoether amino acids do not inhibit DNA damage by Fe(II) (Table 5), but the more strongly binding Pen does. Although quantifiable trends cannot be determined due to lack of IC_{50} values with Fe(II), it is possible that thio- and selenoether ligands do not coordinate Fe(II) strongly enough to prevent iron-mediated DNA damage.

Based on the stability constants of Cu(II) with Met, SeMet, MeCys, MeSeCys, and Gly, the models indicate approximately 100% coordination by at least one ligand at biological pH (Fig. 3). For the Fe(II) stability determinations with the same amino acids, only the Fe(II)-Pen system shows appreciable coordination at biological pH (Fig. 6). These low stability constants reflect the fact that very little Fe(II) is coordinated up to pH 7, although a small change in pH to 8 results in > 80% coordination of Fe(II) as $[ML]^+$ or ML(OH) species. The Fe-Pen system indicates a much higher stability with > 90% coordination at pH 7, indicating probable coordination of the thiolate group to Fe(II). Thus, sulfur and selenium amino acid binding may affect the biological chemistry of Cu(II) significantly more than Fe(II).

4. Conclusions

Stability constants were determined for Cu(II) with the thio- and selenoamino acids Met, MeCys, SeMet, and MeSeCys, and stability constants for the $[Cu(MeSeCys)]^+$ and $Cu(MeSeCys)_2$ species were reported for the first time. Identity of these Cu(II)-amino-acid species were independently confirmed by IR spectroscopy, ESI-MS, and/or solid-state structural analysis, including the first Cu(II) structure with a selenium-containing amino acid, $Cu(SeMet)_2$. Cu(II) binds these amino acids through the amine nitrogen and carboxylate oxygen atoms, and the thioether or selenoether moiety does not coordinate or increase complex stability. Based on the Cu(II) stability constants with these amino acids (log β = 8.0 to 8.2 for the $[ML]^+$ species), all of the available Cu(II) is coordinated at pH 7 as the $[ML]^+$ and $[ML_2]$ species, suggesting that these complexes may potentially form in biological systems.

Stability constants of Fe(II) with MeCys, MeSeCys, and SeMet also were determined for the first time. Fe(II) stability constants are consistently lower than the Cu(II) constants for all sulfur and selenium amino acids tested, including Pen. The $[FeL]^+$ species was identified for all of the thio- and seleno-ether amino acids, consistent with previous reports for the Fe(II)-Met system; however, including a secondary [FeL(OH)] species provided a better match of the model to the titration data. The low stability constants for the $[FeL]^+$ species of the thioether and selenoether amino acids (log β = 3–4) indicate much weaker binding than with Cu(II). As with Cu(II), the similarity of the stability constants for Fe(II) with Gly and all of the thio- and selenoamino acids indicates that the sulfur and selenium atoms do not interact with the metal ion.

In general, the higher stability constants of Cu(II) with the thio- and selenoether amino acids indicates that amino acid binding to Cu(II) at pH 7 may inhibit copper generation of hydroxyl radical, resulting in the weak correlation identified between Cu(II) stability constant and DNA damage prevention abilities of these amino acids. With thio- and selenoether amino acids, the weakly coordinated Fe(II) may be more available than the stronger-binding Cu(II) for redox cycling to generate hydroxyl radical. Although sulfur- and selenium-containing amino acids are considered relatively weakly binding ligands, they may have large-

scale implications for the biological availability and reactivity of redox-active metals such as Cu(II) and Fe(II).

Abbreviations

Asp	L-aspartic acid
Met	L-methionine
Cys	L-cysteine
DNA	deoxyribonucleic acid
EDTA	ethylenediaminetetraacetic acid
EPR	electron paramagnetic resonance
ESI-MS	electrospray ionization mass spectrometry
Gly	glycine
His	L-histidine
hCys	L-homocysteine
HOMO	highest-occupied molecular orbital
IC_{50}	50% inhibitory concentration
ICP-OES	inductively coupled plasma-optical emission spectroscopy
IR	infrared
MeCys	L-methylcysteine
MES	2-(*N*-morpholino)ethanesulfonic acid
MeSeCys	L-methylselenocysteine
MOPS	3-(*N*-morpholino)propanesulfonic acid
NIST	National Institute of Standards and Technology
Pen	L-penicillamine
Phen	1,10-phenanthroline
Pro	L-proline
ROS	reactive oxygen species
SeMet	L-selenomethionine
SeCys	L-selenocysteine
TAE	Tris base, acetic acid, and EDTA
Tris	tris(amino)methane
UV	ultraviolet

Acknowledgements

We thank National Science Foundation grants CHE 1213912 and CHE 1807709 for financial support. J.M.M. thanks Clemson University for a Doctoral Dissertation Completion Grant and Dr. Bradley Stadelman for his synthesis expertise.

Appendix A. Supplementary data

Supplementary data including crystallographic, mass spectrometry, potentiometric titration, and gel electrophoresis data for this article can be found online at https://doi.org/10.1016/j.jinorgbio.2019.03.001. CCDC 1855537 data for $Cu(SeMet)_2$ can be obtained free of charge at http://www.ccdc.cam.ac.uk/conts/retrieving.html.

References

[1] P.S. Hallman, D.D. Perrin, A.E. Watt, Biochem. J. 121 (1971) 549–555.
[2] L.C. Tran-Ho, P.M. May, G.T. Hefter, J. Inorg. Biochem. 68 (1997) 225–231.
[3] G. Berthon, Pure Appl. Chem. 67 (1995) 1117–1240.
[4] G. Berthon, M.J. Blais, M. Piktas, K. Houngbossa, J. Inorg. Biochem. 20 (1984) 113–130.
[5] W.R. Harris, R.D. Sammons, R.C. Grabiak, J. Inorg. Biochem. 116 (2012) 140–150.
[6] M.C. White, Plant Physiol. 67 (1981) 301–310.
[7] L.-C. Konigsberger, E. Konigsberger, G. Hefter, P.M. May, Dalton Trans. 44 (2015) 20413–20425.
[8] S.A. Bellingham, B. Guo, A.F. Hill, Biol. Cell. 107 (2015) 389–418.
[9] M. Mital, N.E. Wezynfeld, T. Fraczyk, M.Z. Wiloch, U.E. Wawrzyniak, A. Bonna, C. Tumpach, K.J. Barnham, C.L. Haigh, W. Bal, S.C. Drew, Angew. Chem. Int. Ed. Engl. 54 (2015) 10460–10464.
[10] A. Kawahara, J. Tsukada, T. Yamaguchi, T. Katsuragi, T. Higashi, Biomark. Res. 3 (2015) 10.
[11] J.M. Mates, J.A. Segura, F.J. Alonso, J. Marquez, Arch. Toxicol. 86 (2012) 1649–1665.
[12] B. Halliwell, J.M. Gutteridge, Methods Enzymol. 186 (1990) 1–85.
[13] K. Jamova, M. Valko, Toxicology 283 (2011) 65–87.
[14] A. Robert, Y. Liu, M. Nguyen, B. Meunier, Acc. Chem. Res. 48 (2015) 1332–1339.
[15] J.T. Brosnan, M.E. Brosnan, J. Nutr. 136 (2006) 1636S–1640S.
[16] A.B. Guttormsen, J. Schneede, T. Fiskerstrand, P.M. Ueland, H.M. Refsum, J. Nutr. 124 (1994) 1934–1941.
[17] J. Bergstroem, P. Fuerst, L. Noree, E. Vinnars, J. Appl. Physiol. 36 (1974) 693–697.
[18] A.M. Kuzminski, E.J. Del Giacco, R.H. Allen, S.P. Stabler, J. Lindenbaum, Blood 92 (1998) 1191–1198.
[19] L.R. Solomon, Blood Rev. 21 (2007) 113–130.
[20] J. Selhub, Annu. Rev. Nutr. 19 (1999) 217–246.
[21] P.R. Mandaviya, L. Stolk, S.G. Heil, Mol. Genet. Metab. 113 (2014) 243–252.
[22] L. Hoey, H. McNulty, N. Askin, A. Dunne, M. Ward, K. Pentieva, J. Strain, A.M. Molloy, C.A. Flynn, J.M. Scott, Am. J. Clin. Nutr. 86 (2007) 1405–1413.
[23] T. Selmer, J. Kahnt, M. Goubeaud, S. Shima, W. Grabarse, U. Ermler, R.K. Thauer, J. Biol. Chem. 275 (2000) 3755–3760.
[24] F.M. Rubino, M. Pitton, D. Di Fabio, G. Meroni, E. Santaniello, E. Caneva, M. Pappini, A. Colombi, Biomed. Chromatogr. 25 (2011) 330–343.
[25] G.J. Brewer, Drugs 50 (1995) 240–249.
[26] G.J. Brewer, F.K. Askari, J. Hepatol. 42 (2005) S13–S21.
[27] M. Shannon, J. Graef, F.H. Lovejoy Jr., J. Pediatr. 112 (1988) 799–804.
[28] A.O. Muijsers, R.J. van de Stadt, A.M.A. Henrichs, H.J.W. Ament, J.K. van der Korst, Arthritis Rheumatol. 27 (1984) 1362–1369.
[29] R.F. Burk, B.K. Norsworthy, K.E. Hill, A.K. Motley, D.W. Byrne, Cancer Epidemiol. Biomark. Prev. 15 (2006) 804–810.
[30] M.E. Reid, M.S. Stratton, A.J. Lillico, M. Fakih, R. Natarajan, L.C. Clark, J.R. Marshall, J. Trace Elem. Med. Biol. 18 (2004) 69–74.
[31] K. Takahashi, N. Suzuki, Y. Ogra, Int. J. Mol. Sci. 18 (2017) 506–517.
[32] B.J. Byun, Y.K. Kang, Biopolymers 95 (2011) 345–353.
[33] M. Kotrebai, M. Birringer, J.F. Tyson, E. Block, P.C. Uden, Analyst 125 (2000) 71–78.
[34] R.F. Burk, K.E. Hill, Annu. Rev. Nutr. 25 (2005) 215–235.
[35] R.F. Burk, K.E. Hill, Biochim. Biophys. Acta 1790 (2009) 1441–1447.
[36] S.J. Fairweather-Tait, Y. Bao, M.R. Broadley, R. Collings, D. Ford, J.E. Hesketh, R. Hurst, Antioxid. Redox Signal. 14 (2011) 1337–1383.
[37] L.V. Papp, A. Holmgren, K.K. Khanna, Antioxid. Redox Signal. 12 (2010) 793–795.
[38] E.E. Battin, M.T. Zimmerman, R.R. Ramoutar, C.E. Quarles, J.L. Brumaghim, Metallomics 3 (2011) 503–512.
[39] M.B. Colovic, V.M. Vasic, D.M. Djuric, D.Z. Krstic, Curr. Med. Chem. 25 (2018) 324–335.
[40] A. Gonzalez-Benjumea, P. Begines, O. Lopez, I. Maya, J.G. Fernandez-Bolanos, Adv. Chem. Res. 22 (2014) 51–81.
[41] S. Metayer, I. Seiliez, A. Collin, S. Duchene, Y. Mercier, P.A. Geraert, S. Tesseraud, J. Nutr. Biochem. 19 (2008) 207–215.
[42] A.S. Rahmanto, M.J. Davies, IUBMB Life 64 (2012) 863–871.
[43] S. Palioura, J. Herkel, M. Simonovic, A.W. Lohse, D. Soll, Biol. Chem. 391 (2010) 771–776.
[44] J. Liu, Y. Zhao, R. Zhang, J. Shu, X. Zhang, Zhongguo Shipin Tianjiaji 2 (2011) 152–156.
[45] E.E. Battin, J.L. Brumaghim, J. Inorg. Biochem. 102 (2008) 3036–3042.
[46] M.T. Zimmerman, C.A. Bayse, R. Ramoutar, J.L. Brumaghim, J. Inorg. Biochem. 145 (2015) 30–40.
[47] B.S. Stadelman, M.M. Kimani, C.A. Bayse, C.D. McMillen, J.L. Brumaghim, Dalton Trans. 45 (2016) 4697–4711.
[48] P. Gans, A. Sabatini, A. Vacca, Talanta 43 (1996) 1739–1753.
[49] Apex3, Bruker AXS Inc., Madison, WI, 2015.
[50] G.M. Sheldrick, Acta Cyrstallogr. C71 (2015) 3–8.
[51] R.S. Lloyd, C.W. Haidle, D.L. Robberson, Biochemistry 17 (1978) 1890–1896.
[52] R.P. Hertzberg, P.B. Dervan, J. Am. Chem. Soc. 104 (1982) 313–315.
[53] F. Basolo, Y.T. Chen, J. Am. Chem. Soc. 76 (1954) 953–955.
[54] I. Sovago, T. Kiss, A. Gergely, Pure Appl. Chem. 65 (1993) 1029–1080.
[55] H. Zainal, W. Wolf, Transit. Met. Chem. 20 (1995) 225–227.
[56] A. Albert, Biochem. J. 47 (1950) 531–538.
[57] N.C. Li, E. Doody, J. Am. Chem. Soc. 76 (1954) 221–225.
[58] C.J. Hawkins, D.D. Perrin, Inorg. Chem. 2 (1963) 843–849.
[59] V. Jokl, J. Chromatogr. 14 (1964) 71–78.
[60] G. Lenz, A. Martell, Biochemistry 3 (1964) 745–750.
[61] P.A. Pella, W.C. Purdy, J. Electroanal. Chem. 10 (1965) 51–55.
[62] G. Brookes, L.D. Pettit, J. Chem. Soc. Dalton Trans. (1977) 1918–1924.
[63] K. Prasad, M.S. Mohan, J. Coord. Chem. 16 (1987) 251–262.
[64] M.S. Masoud, B.A. Abdel-Nabby, E.M. Soliman, O.H. Abdel-Hamid, Thermochim. Acta 128 (1988) 75–80.
[65] Z.M. Anwar, H.A. Azab, J. Chem. Eng. Data 44 (1999) 1151–1157.
[66] A. Albert, Biochem. J. 50 (1952) 690–697.
[67] E.C. Knoblock, W.C. Purdy, J. Electroanal. Chem. 2 (1961) 493–496.
[68] P. Deschamps, P.P. Kulkarni, B. Sarkar, Inorg. Chem. 43 (2004) 3338–3340.
[69] L. Antolini, L.P. Battaglia, C.A. Bonamartini, G. Marcotrgiano, L. Menabue, G.C. Pellacani, M. Saladini, M. Sola, Inorg. Chem. 26 (1986) 2901–2904.
[70] K. Tomita, Bull. Soc. Chim. Jpn. 34 (1961) 297–300.
[71] G. Borghesani, F. Pulidori, M. Remelli, R. Purrello, E. Rizzarelli, J. Chem. Soc. Dalton Trans. (1990) 2095–2100.
[72] M. Israeli, L.D. Pettit, J. Inorg. Nucl. Chem. 37 (1975) 999–1003.
[73] I. Sovago, G. Petocz, J. Chem. Soc. Dalton Trans. (1987) 1717–1720.
[74] L.D. Pinto, P. Puppin, V.M. Behring, O. Alves, N. Rey, J. Felcman, Inorg. Chim. Acta 386 (2012) 60–67.
[75] E.J. Kuchinkas, Y. Rosen, Arch. Biochem. Biophys. 97 (1962) 370–372.
[76] A. Gergely, Acta Chim. Acad. Sci. Hung. 59 (1969) 309–318.
[77] D.D. Perrin, J. Chem. Soc. (1958) 3125–3128.

[78] D.A. Doornbos, J.S. Faber, Pharm. Weekbl. 99 (1964) 289–309.
[79] C. Ou, D. Powers, J. Thich, T. Felthouse, D. Hendrickson, J. Potenza, H. Schugar, Inorg. Chem. 17 (1978) 34–40.
[80] E. Dubler, N. Cathomas, G.B. Jameson, Inorg. Chim. Acta 123 (1986) 99–104.
[81] M.S. Masoud, M.F. Amira, A.M. Ramadan, G.M. El-AShry, Spectrochim. Acta 69A (2008) 230–238.
[82] M. Veidis, G. Palenik, J. Chem. Soc. D 21 (1969) 1277–1278.
[83] S. Yoneyama, T. Kodama, K. Kikuchi, Y. Kawabata, K. Kikuchi, T. Ono, Y. Hosokoshi, W. Fujita, CrystEngComm 15 (2013) 10193–10196.
[84] C.K. Prout, R.A. Armstrong, J.R. Carruthers, J.G. Forrest, P. Murray-Rust, F. Rossotti, J. Chem. Soc. A 11 (1968) 2791–2813.
[85] H.C. Freeman, M.R. Snow, I. Nitta, K. Tomita, Acta Crystallogr. 17 (1964) 1463–1470.
[86] B.M. Casari, A.H. Mahmoudkhani, V. Langer, Acta Crystallogr. E60 (2004) m1949–m1951.
[87] S. Konar, K. Gagnon, A. Clearfield, C. Thompson, J. Hartle, C. Ericson, C. Nelson, J. Coord. Chem. 63 (2010) 3335–3347.
[88] M. Lamshoft, B. Ivanova, J. Coord. Chem. 64 (2011) 2419–2442.
[89] A. Gergely, I. Sóvágó, Bioinorg. Chem. 9 (1978) 47–60.
[90] I. Sóvágó, B. Harman, A. Gergely, Inorg. Chim. Acta 46 (1980) L107–L108.
[91] N. Yoshinari, A. Kakuya, R. Lee, T. Konno, Bull. Chem. Soc. Jpn. 88 (2015) 59–68.
[92] D.D. Perrin, J. Chem. Soc. (1959) 290–296.
[93] R.M. Izatt, H.D. Johnson, J.J. Christensen, J. Chem. Soc. Dalton Trans. 11 (1972) 1152–1157.
[94] K. Micskei, J. Chem. Soc. Dalton Trans. (1987) 255–257.
[95] C.P. Magill, C. Floriani, A. Chiesi-Villa, C. Rizzoli, Inorg. Chem. 33 (1994) 1928–1933.
[96] N.D. Jhurry, M. Chakrabarti, S.P. McCormick, G.P. Holmes-Hampton, P.A. Lindahl, Biochemistry 51 (2012) 5276–5284.
[97] L. Yang, R. McRae, M.M. Henary, R. Patel, B. Lai, S. Vogt, C.J. Fahrni, Proc. Natl. Acad. Sci. U. S. A. 102 (2005) 11179–11184.
[98] C.J. Fahrni, Curr. Opin. Chem. Biol. 17 (2013) 656–662.
[99] E. Gaggelli, H. Kozlowski, D. Valensin, G. Valensin, Chem. Rev. 106 (2006) 1995–2044.
[100] E.E. Battin, N.R. Perron, J.L. Brumaghim, Inorg. Chem. 45 (2006) 499–501.
[101] C.R. Garcia, C. Angele-Martinez, J.A. Wilkes, H.C. Wang, E.E. Battin, J.L. Brumaghim, Dalton Trans. 41 (2012) 6458–6467.